Increased in vitro neutralizing activity of SARS-CoV-2 IgA1 dimers compared to monomers and IgG

Lin Sun[a,1], Somanath Kallolimath[a,1,2], Roman Palt[a], Karin Stiasny[b], Patrick Mayrhofer[c], Daniel Maresch[d], Lukas Eidenberger[a], and Herta Steinkellner[a,3]

[a]Department of Applied Genetics and Cell Biology, University of Natural Resources and Life Sciences, 1190 Vienna, Austria; [b]Center for Virology, Medical University of Vienna, 1090 Vienna, Austria; [c]Department of Biotechnology, University of Natural Resources and Life Sciences, 1190 Vienna, Austria; and [d]Core Facility Mass Spectrometry, University of Natural Resources and Life Sciences, 1190 Vienna, Austria

Here, we expressed two neutralizing monoclonal antibodies (Abs) against severe acute respiratory syndrome coronavirus 2 (SARS-CoV-2; H4 and B38) in three formats: IgG1, IgA1 monomers (m), and IgA1 dimers (d) in glycoengineered *Nicotiana benthamiana* plants. All six Ab variants assembled properly and exhibited a largely homogeneous glycosylation profile. Despite modest variation in antigen binding between Ab formats, SARS-CoV-2 neutralization (NT) potency significantly increased in the following manner: IgG1 < IgA1-m < IgA1-d, with an up to 240-fold NT increase of dimers compared to corresponding monomers. Our results underscore that both IgA's structural features and multivalency positively impact NT potency. In addition, they emphasize the versatile use of plants for the rapid expression of complex human proteins.

monoclonal antibodies | plant expression | SARS-CoV-2 | IgA

Severe acute respiratory syndrome coronavirus 2 (SARS-CoV-2)–specific IgA1 variants have been shown to neutralize more efficiently than their IgG and IgM counterparts (1). Interestingly, dimeric IgA, the primary form of antibody in the nasopharynx, was reported to be more potent than IgA monomers against the same target (2). Despite the known diverse activities of IgA in viral host defense, the roles of these various molecular forms are not yet well defined. Here, we focused on the *in planta* production and functional characterization of glycoengineered IgA1 variants against SARS-CoV-2 in comparison with the IgG1 orthologs.

Results

Monoclonal B38 and H4 IgG1 and IgA1 Variants. Two SARS-CoV-2 neutralizing monoclonal IgG1 antibodies, H4 and B38 (3), served as templates in this study. Four plant expression constructs representing IgG1 and IgA1 isotypes were generated (*H4/B38-IgG1* and *H4/B38-IgA1*) (*SI Appendix*). Respective constructs were delivered into *Nicotiana benthamiana* glycosylation mutant ΔXTFT (4) by agroinfiltration. IgA1 constructs were coinfiltrated with the joining chain (JC) to promote the *in planta* generation of dimers and oligomers (5). Antibodies were immunoaffinity purified followed by analytical size exclusion chromatography with multiangle light scattering (SEC-MALS). Distinct peaks with a mass of ~150 kDa, corresponding to the theoretical mass of IgA1 monomers, were observed. In addition, overlapping peaks with a molecular mass of ~350 and ≥715 kDa were detected, representing dimers (including joining chain) and possibly higher-order IgA1 molecular forms (Fig. 1*A*). The different IgA1 molecular forms were isolated by preparative SEC and analyzed by nonreducing gradient gel separation (Fig. 1*B*). In total, three variants from each, H4 and B38, were generated: IgG1, IgA1 monomers (m), and dimers (d). Sodium dodecyl sulfate polyacrylamide gel electrophoresis (SDS/PAGE) of purified IgA1 under reducing conditions (irrespective which molecular form) confirmed the presence of the LC and HC without degradation products or other impurities (Fig. 1 *B*, *Right*).

Plant-Produced Abs Exhibit a Homogeneous Glycosylation Profile. Since recent results demonstrate glycosylation-dependent functional effects of antibodies in infectious diseases, including COVID-19 (6, 7), we aimed at the production of Abs with targeted largely homogenous glycosylation profiles. Fc domains of IgG1 and IgA1 exhibit one and two conserved *N*-glycosites (GS), respectively. Liquid chromatography–electrospray ionization–tandem mass spectrometry (LC-ESI-MS/MS) of B38-IgA1 and H4-IgA1 revealed that, in both sites, most *N*-glycans terminate with one or two GlcNAc residues (GnGn and MGn structures 50 to 80% at the NLT site and 40 to 60% at the NVS site; Fig. 1*C*), as expected by using the glycosylation mutant ΔXTFT (4). Notably, at the NVS site, up to 20% fucose-carrying *N*-glycans are present. Overall, compared to mammalian cell-produced IgA versions with >30 glycoforms (8), the plant-generated orthologs exhibited a largely homogeneous glycosylation profile. The single Fc GS of IgG1 exhibited >90% GnGn structures (Fig. 1*C*).

Antigen Binding and Neutralization Potency of Dimeric vs. Monomeric IgA1. To examine the antigen-binding properties of the antibodies, we performed ELISAs with the SARS-CoV-2 spike protein homotrimer (SP; further details in *SI Appendix*). As reported earlier (3), H4-IgG1 exhibited better binding than B38-IgG1 (effective concentration, 50% [EC_{50}] 0.29 and 1.55 nM, respectively; Table 1). Comparing the three Ab formats of H4, we observed similar binding of all three variants (EC_{50} 0.29, 0.28, and 0.19 nM, respectively; Table 1). In accordance, B38 IgG1 and IgA1-m exhibited similar binding behaviors (EC_{50} 1.55 and 1.38 nM, respectively); however, IgA1-d showed increased binding properties (EC_{50} 0.2 nM), suggesting epitope-specific activities of these Abs.

To determine functional activities of Ab variants, virus neutralization (NT) assays were performed, as described previously (9) and in *SI Appendix*. Using H4, we observed fivefold higher activity of IgA1-m than of IgG1 (NT_{100} 24.20 and 123.30 nM, respectively), and another 48-fold increase for IgA1-d (NT_{100} 0.50 nM). This finally corresponds to a ~240 times superior NT potency of IgA1-d compared with IgG1 (Table 1). A similar trend was observed with B38 Ab formats. We saw a 33-fold NT increase comparing IgA1-m with IgA1-d (NT_{100} 298.80 and 8.85 nM,
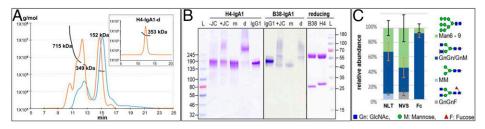
Fig. 1. (*A*) SEC-MALS profiles of IgA1: overlay of B38-IgA1 (blue line) and H4-IgA1 (orange line); *Inset* represents SEC isolated H4-IgA1 dimers (~353 kDa); *x* axis is retention time (minutes), and *y* axis is molar mass (grams per mole) (numbers represent B38 variants: ~152-kDa monomers, ~349-kDa dimers, and ≥715-kDa oligomers/aggregates). (*B*) (*Left* and *Middle*) Nonreducing gradient gel (4 to 20%, Commassie brilliant blue stained) of purified H4-IgA1 and B38-IgA1 with and without JC (+JC and −JC); m, SEC isolated monomers; d, dimers. H4-IgG1 and B38-IgG1 (IgG1) were used as control. (*Right*) Representative SDS/PAGE (12%, under reducing conditions) of purified B38-IgA1 (B38) and H4-IgA1 (H4); L, protein ladder. (*C*) LC-ESI-MS/MS–derived glycosylation profiles of IgA1 and IgG1 produced in ΔXTFT. Bars represent the relative abundance (percent) of glycoforms present at each GS [IgA1: 263NLT and 459NVS, IgG1: 297NST (Fc)]. Nomenclature is according to Consortium for Functional Glycomics.

respectively). The NT activity of B38-IgG1 was ≥678 nM (Table 1).

When using mass concentration EC_{50} and NT_{100} values (microgram per milliliter) instead of molarities, we obtained some deviations comparing monomeric with dimeric Abs, for example, only a ~20-fold increase of NT for IgA1-m vs. IgA1-d (Table 1).

Discussion

Our studies underpin the versatile activities of SARS-CoV-2–specific antibodies and emphasize the importance of IgA1 molecular forms. Interestingly, while we did not observe significant variation in antigen binding between the H4 Ab formats in ELISA, an up to 240 times higher NT ability was obtained between the monomeric and the dimeric formats. Due to the low NT activity of B38-IgG1, we were not able to draw a clear activity line. However, with NT_{100} ≥ 678 of B38-IgG1, we anticipate an at least ~70-fold NT increase of B38-IgA1-d (NT_{100} 8.85 nM). Both H4-IgA1-m and B38-IgA1-m exhibited a 30- to 50-fold decreased NT ability compared to the dimeric forms, while only a fivefold difference was observed comparing H4-IgG1 and H4-IgA1-m. The data suggest that both structural features (e.g., long hinge region) and multivalency of IgA1 positively impact NT potency. However, superior activity seems to be more associated with oligomerization than with the isotype switch, which corroborates the bonus effect of Ab multivalency that defines avidity not as the simple sum of individual binding site affinities (10, 11). Superior NT potency of the IgA1-d compared to modest antigen-binding variations of monomeric counterparts in ELISA suggests that cross-linking the S protein on the viral surface might be responsible for enhanced neutralizing activity rather than increased antigen-binding abilities, in agreement with recent studies on SARS-CoV-2 IgG3 mAbs (12). Our results are in line with previous reports demonstrating potent NT by IgA variants in viral settings (2, 10) and may be considered in therapy and vaccine development. Notably, here, Ab variants with relatively low NT potencies were expressed. In the case of drug development, Abs with higher potencies (in the subnanomolar range) may be used.

Collectively, we describe the rapid *in planta* expression of a series of complex human proteins (Ab collection 4 d post DNA construct delivery) of sudden need. Nevertheless, it should be mentioned that the incomplete formation of IgA dimers may provide a challenge for large-scale biomanufacturing approaches. The expression of Ab variants with a highly homogeneous glycosylation profile, reflecting the core eukaryotic *N*-glycan structure (GnGn/G0), provides an excellent basis for further Ab glycan engineering (13) to elucidate so far potentially unknown glycosylation-dependent activities of SARS-CoV-2 antibodies, as suggested recently (6, 7).

Materials and Methods

In planta expression of IgA1 antibodies was performed by agroinfiltration (5). Affinity-purified IgA1 mAbs were fractionated by SEC to obtain monomer and dimers. Fractions were subjected to ELISA antigen-binding assay, and NT assay using vero cells was performed as described in ref. 9. Materials and methods are detailed in *SI Appendix*.

Data Availability. All study data are included in the article and *SI Appendix*.

Table 1. ELISA binding activities to SP (EC_{50} values) using respective anti-HC antibodies for detection and SARS-CoV-2 NT activities (NT_{100} values) of antibody variants

Ab (target SP)	EC_{50} (nM)	EC_{50} (ng/mL)	NT_{100} (nM)	NT_{100} (μg/mL)
H4-IgG1	0.29	50.00	123.30	18.75
H4-IgA1-m	0.28	43.00	24.20	3.75
H4-IgA1-d	0.19	61.00	0.50	0.16
B38-IgG1	1.55	251.00	≥678.00	≥100.00
B38-IgA1-m	1.38	207.80	298.80	45.00
B38-IgA1-d	0.20	63.30	8.85	2.88

1. W. Zeng *et al.*, Characterization of SARS-CoV-2-specific antibodies in COVID-19 patients reveals highly potent neutralizing IgA. *Signal Transduct. Target. Ther.* **6**, 35 (2021).
2. Z. Wang *et al.*, Enhanced SARS-CoV-2 neutralization by dimeric IgA. *Sci. Transl. Med.* **13**, eabf1555 (2021).
3. Y. Wu *et al.*, A noncompeting pair of human neutralizing antibodies block COVID-19 virus binding to its receptor ACE2. *Science* **368**, 1274–1278 (2020).
4. R. Strasser *et al.*, Generation of glyco-engineered *Nicotiana benthamiana* for the production of monoclonal antibodies with a homogeneous human-like *N*-glycan structure. *Plant Biotechnol. J.* **6**, 392–402 (2008).
5. A. Loos *et al.*, Expression and glycoengineering of functionally active heteromultimeric IgM in plants. *Proc. Natl. Acad. Sci. U.S.A.* **111**, 6263–6268 (2014).
6. S. Chakraborty *et al.*, Proinflammatory IgG Fc structures in patients with severe COVID-19. *Nat. Immunol.* **22**, 67–73 (2021).
7. M. D. Larsen *et al.*, Afucosylated IgG characterizes enveloped viral responses and correlates with COVID-19 severity. *Science* **371**, eabc8378 (2021).
8. K. Göritzer, D. Maresch, F. Altmann, C. Obinger, R. Strasser, Exploring site-specific *N*-glycosylation of HEK293 and plant-produced human IgA isotypes. *J. Proteome Res.* **16**, 2560–2570 (2017).
9. M. Koblischke *et al.*, Dynamics of CD4 T cell and antibody responses in COVID-19 patients with different disease severity. *Front. Med. (Lausanne)* **7**, 592629 (2020).
10. A. W. Freyn *et al.*, Influenza hemagglutinin-specific IgA Fc-effector functionality is restricted to stalk epitopes. *Proc. Natl. Acad. Sci. U.S.A.* **118**, e2018102118 (2021).
11. K. B. Renegar, G. D. Jackson, J. Mestecky, In vitro comparison of the biologic activities of monoclonal monomeric IgA, polymeric IgA, and secretory IgA. *J. Immunol.* **160**, 1219–1223 (1998).
12. S. Kallolimath *et al.*, Highly active engineered IgG3 antibodies against SARS-CoV-2. *Proc. Natl. Acad. Sci. U.S.A.* **118**, e2107249118 (2021).
13. L. Montero-Morales, H. Steinkellner, Advanced plant-based glycan engineering. *Front. Bioeng. Biotechnol.* **6**, 81 (2018).

2 of 2 | PNAS
https://doi.org/10.1073/pnas.2107148118

Sun et al.
Increased in vitro neutralizing activity of SARS-CoV-2 IgA1 dimers compared to monomers and IgG